



# Linkage of tropical glaciation to supercontinents: a thermodynamic closure model

Hsien-Wang Ou<sup>1</sup>

<sup>1</sup> Lamont-Doherty Earth Observatory, Columbia University, Palisades, NY 10964, USA

5 *Correspondence to:* H.-W. Ou (hsienou0905@gmail.com)

**Abstract.** Precambrian tropical glaciations pose a significant challenge to our understanding of Earth's climate. A popular explanation invokes runaway ice-albedo feedback leading to "iceball earth", an extreme state conflicting however with the sedimentary evidence of an open ocean and active hydrological cycle. We point out flawed physics of the runaway scenario, which overlooks potency of the ocean heat transport in deterring the perennial sea ice. Nor is frozen ocean needed for tropical  
10 glaciation as the latter requires only that the tropical land be cooled to below the marking temperature of the glacial margin, which is necessarily above the freezing point to counter the yearly accumulation. Since tropical glaciations generally coincide with Precambrian supercontinents, we posit that it is their blockage of the brighter tropical sun that causes the required cooling. To test this hypothesis, we formulate a minimal two-box model, which is nonetheless thermodynamically closed and yields lowering tropical/polar temperatures with increasing tropical land, whose crossings of the glacial marking temperature would  
15 divide non/polar/pan-glacial regimes—the last being characterized by tropical glaciation abutting an open ocean. Given the observed chronology of paleogeography, our theory may provide a unified account of the faint-young-sun paradox, Precambrian tropical glaciations and glacio-epochs through Earth's history.

## 1 Introduction

Cryogenian glacio-epochs stand out in that glaciers have advanced to the sea level in the tropics (Chumakov & Elston, 1989;  
20 Sohl et al., 1999; Evans, 2003; Kilner et al., 2005), a pan-glacial state coined "snowball earth" by Kirschvink (1992) without implicating a frozen ocean. Invoking runaway ice-albedo feedback and peculiar glacial sequence, Hoffman et al. (1998) proposes an extreme interpretation of the tropical glaciation by way of an ice-covered planet, which we shall refer to as "iceball earth" for distinction (Harland, 2007)—avoiding the misnomer of "snow" over a global frozen ocean. The iceball earth hypothesis has largely been refuted by sedimentary evidence: the putative tell-tale signs of cap carbonates and iron formation  
25 turn out to be nonunique to a global frozen ocean (Kennedy et al., 2001; Jiang et al., 2003; Le Guerrouè et al., 2006; Fairchild & Kennedy 2007; Etinne et al., 2007; Eyles, 2008) and dynamic glacial advance/retreat indicates an active hydrological cycle predicated on an open ocean (Christie-Blick et al., 1999; Condon et al., 2002; Leather et al., 2002; Rieu et al., 2007; Chumakov, 2008; Allen & Etienne, 2008). Given extensive literature on the glacial sedimentology, our focus is on the physics of the tropical glaciation, and in this introduction, we shall point out flawed physics of past models, pertaining particularly to glacial



30 margin, ocean heat transport (OHT),  $p\text{CO}_2$  and cloud in successive paragraphs below, and preview their possible remedies in our model.

We begin with the energy-balance model, a progenitor of the runaway ice-albedo feedback, which presupposes a common land/sea-ice line taggable by temperature (Budyko, 1969)—overlooking a fundamental difference of the two media in that the ocean can transport heat. While one may tag the land-ice margin by the summer surface-air temperature (SAT), which controls the ablation, this temperature nonetheless should be above the freezing point to counter the yearly accumulation, and since summer isotherms are predominantly zonal (Sect. 3), the glacial margin thus should abut an open ocean. This argument is consistent with the present Greenland ice sheet protruding into the open North Atlantic and the Laurentide ice sheet of the last ice age extending into the subtropics, and it is the reason that climate models incorporating the ice-sheet dynamics have produced a more expansive land ice (Hyde et al., 2000). By extension, the land ice would advance into the tropics so long as the tropical land is cooled to below this marking temperature—without a frozen ocean premised in iceball earth (Yang et al., 2012).

For the sea ice, on the other hand, a freezing-point surface provides only a necessary condition for ice formation, which can be sustained (perennial) only if the OHT may not overcome the yearly cooling. Here we come upon an Achilles heel in climate modeling: OHT obviously cannot be properly captured by slab, mixed-layer or diffusive ocean models (Jenkins & Smith, 1999; Chandler & Sohl, 2000; Bice et al., 2000; Poulsen et al., 2001; Donnadieu et al., 2004; Braun et al., 2022; Hörner et al., 2022), but even in (coarse-grained) primitive-equation models, OHT depends critically on diapycnal diffusivity, which is in effect a free parameter finely tuned to produce the present climate (Bendtsen, 2002; Rahmstorf et al., 2005) and, being a free parameter, there is no reason that the tuned value should apply to a vastly different paleoclimate. We attribute this nonclosure to coarse-graining of the meridional overturn circulation (MOC), which takes the form of a laminar overturning cell, whereas the actual one is composed partly of random eddies (Lozier, 2010) to be subjected to probability laws of the nonequilibrium thermodynamics (NT). Resolving eddies obviously poses a daunting challenge to the numerical simulation of glacio-epochs, which points to a palpable advantage of our theoretical construct unrestrained by computing resources—not to mention its faculty in elucidating the underlying physics. We should note that even rudimentary treatment of OHT by aforementioned models has significantly curbed the sea-ice advance, and some simulations of the runaway scenario are actually artifacts of an unbalanced initial state (Voigt et al., 2010; Yang et al., 2012) when OHT simply has no time to act in deterring the sea ice.

Besides the need to include ice-sheet dynamics and OHT, a common yet questionable practice of climate modelling is in prescribing internal properties of the climate system to probe its response. A prominent example is  $p\text{CO}_2$  (Pollard & Kasting, 2004; Pierrehumbert et al., 2011), which would feedback negatively on temperature to equilibrate over a million-year (Walker et al., 1981; Brady & Carroll, 1994; Berner & Caldeira, 1997; Godderis & Donnadieu, 2019) hence cannot be independently prescribed on tectonic timescale. For such timescale,  $p\text{CO}_2$  is poorly constrained by proxy data and is among the least correlative climate indicators (Boucot & Gray, 2001; Eyles, 2008), yet it is conveniently invoked to cure many climate puzzles, including “faint-young-sun paradox” (FYSP, Crowley & North, 1991) and tropical glaciations (Pierrehumbert et al., 2011).



65 However uncertain,  $p\text{CO}_2$  reconstructed from paleosols falls far short in countering the dimmer sun (Sheldon et al., 2021) and even if it were sufficient, one still needs to explain why it would settle on this particular level that enables a habitable planet. In addition,  $p\text{CO}_2$  remains relatively steady through Neoproterozoic, displaying no wild swings envisaged by iceball earth (Sansjofre et al., 2011; Sheldon et al., 2021).

70 Another key internal variable lost amidst overprescribed  $p\text{CO}_2$  is the cloud: while three orders-of-magnitude greater  $p\text{CO}_2$  than the present is needed to counter the dimmer sun (Kasting, 1993), a mere 30% reduction in cloud is sufficient. Unlike  $p\text{CO}_2$ , cloud has no proxy data, which moreover is not subjected to budget constraint as its generation/dissipation involves cloud physics of practically infinitive degrees of freedom. Clearly, unless the cloud is constrained by global thermodynamics, one does not have an explanation of Earth's temperature; for this reason, we shall retain only cloud to provide the requisite internal degree of freedom for our model closure. We should stress that absent a physical closure, no amount of outward sophistication of a climate model may advance its prognosis. Nor may such a model arbitrate our closure theory, which should  
75 be adjudicated only by its logical soundness and observation.

Since tropical glaciations are characterized by tectonic timescale, whatever their governing physics should also be operative for FYSP, we stipulate therefore that a valid thermodynamic closure must accommodate both phenomena and that they can be differentiated only by external condition. This uniformitarian view arguably precludes the runaway ice-albedo feedback since its triggering threshold is amply exceeded by the dimmer sun in Proterozoic, which however is largely free of  
80 glaciations. As for discernible external condition, we take note that tropical glaciations generally coincide with Precambrian supercontinents (Eyles, 2008; Williams et al., 2016) to posit that their concentration of the tropical landmass would block the brighter tropical sun to cause the required cooling.

To test this hypothesis in a most transparent manner, we construct a minimal box model, whose thermodynamic closure is first discussed in Sect. 2, to be followed in Sect. 3 by the derivation of glacial regimes. Given the observed paleogeography,  
85 we then apply the model prognosis in Sect. 4 to interpret glacio-epochs through Earth's history. We summarize the main findings in Sect. 5 to conclude the paper.

## 2 Thermodynamic Closure

Because of inherently turbulent nature of the planetary fluids, the climate is a macroscopic manifestation of a NT system hence likely subjected to maximum entropy production (MEP)—a generalized second law (Ozawa et al., 2003; Kleidon, 2009). Its  
90 predicate here on turbulence renders moot some its previous criticisms (Bruers, 2007) whose physical basis is further strengthened by its linkage to the fluctuation theorem (Dewar, 2005; Martyushev & Seleznev, 2006; Ou, 2018) as the latter is of considerable mathematical rigor and has been tested in the laboratory (Evans & Searle, 2002; Wang et al., 2002). For computational supports, MEP has emerged from general circulation models (Shimokawa & Ozawa, 2002; Kleidon et al., 2003) and eddy-resolving and direct numerical simulations of horizontal convection (Hogg & Gayen, 2020; Liu et al., 2022) have  
95 reproduced its signature feature (a mid-latitude front, Ou, 2006) absent from coarse-grained numerical models (Colin de



Verdière, 1988). In addition, MEP has replicated broad climate features and resolved some long-standing climate puzzles (Paltridge, 1975; Lorenz et al., 2001; Ou, 2023a).

With above supports, we have invoked MEP in our previous derivation of the generic climate state from first principles (Ou, 2001, 2006). The formulation is aided by the recognition that MEP is a selection rule hence can be applied hierarchically (Lucarini et al., 2011)—first to the global-mean and then to the latitudinal fields, and since turbulence is internal to the fluids, MEP should apply to atmosphere and ocean individually. With the thermodynamic closure, certain derived climate properties may be regarded as known, which are first articulated below for the completeness of the present theory.

Through a global-mean model of aquaplanet, Ou (2001) demonstrates that clouds would self-adjust to stabilize the surface temperature constrained by intrinsic water properties. To illustrate this constraint, let us suppose that for a given forcing, variable clouds allow a continuum surface temperature ( $\bar{T}$ ) spanning the x-axis (linear in the corresponding blackbody radiance) of Fig. 1 and as an intrinsic water property, the saturation vapor pressure ( $e$ ) rises increasingly sharply with warming surface (Clausius–Clapeyron relation). The accompanying long-wave (LW) absorption would increasingly differentiate surface ( $q_{surf}$ ) and outgoing ( $q_{OLR}$ ) LW fluxes (the greenhouse effect) to augment the LW cooling of the atmosphere (shaded, all radiative fluxes normalized by one-quarter of the present solar constant), which must be countered by increasing convective flux from the surface ( $q_c$ ). This convective flux is proportional to the product of turbulent wind ( $u'$ ) and sea/air difference in the moist static energy, the latter roughly trending as the vapor pressure—except a finite cold asymptote because of the sensible heat. As such, the turbulent wind (thick line) first increases with the greenhouse warming, then decreases by the rising vapor pressure to render a local maximum (solid square). Since the turbulent wind varies with the frictional dissipation hence irreversible entropy production (Ou, 2001; Kleidon et al., 2014), MEP thus selects a temperature constrained by the intrinsic water properties.

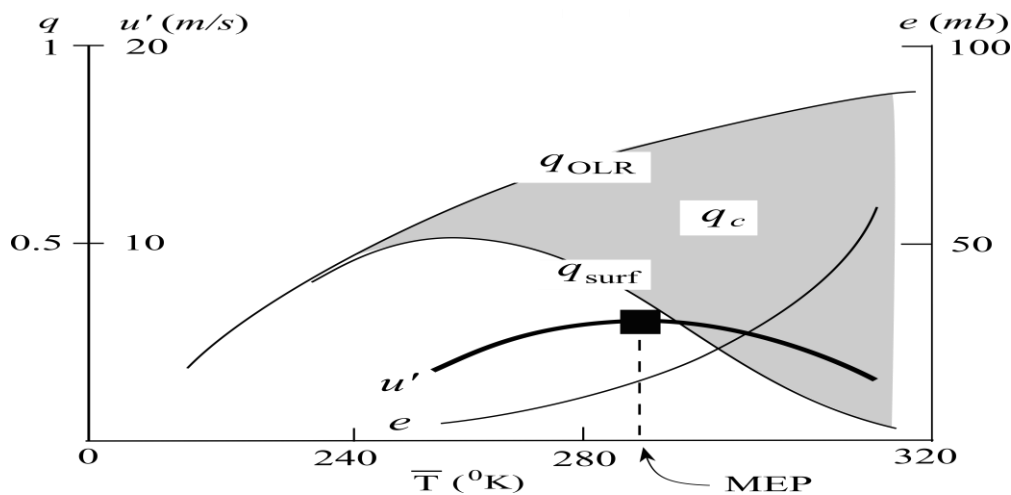


**Figure 1.** A schematic in which the saturation vapor pressure ( $e$ ), LW fluxes ( $q$ 's, normalized by one-quarter of the present solar constant), convective flux ( $q_c$ , shaded), and turbulent wind ( $u'$ ) are plotted against the surface temperature ( $\bar{T}$ , linear in the corresponding blackbody radiance). The maximum  $u'$  (solid square) selects the MEP temperature.



120 Quantitatively, it is found that a 30% decrease of the solar insolation (about  $100 \text{ Wm}^{-2}$ ) would be buffered by varying clouds to incur only  $20 \text{ Wm}^{-2}$  reduction in the absorbed SW flux ( $\bar{q}$ ) accompanied by  $10 \text{ }^\circ\text{C}$  global cooling, resulting in a sensitivity of

$$s \equiv \delta\bar{T}/\delta\bar{q} \approx 0.5 \text{ }^\circ\text{C}(\text{Wm}^{-2})^{-1}, \quad (1)$$

an often-quoted value (Pierrehumbert et al., 2011). It is seen therefore that so long as there is ocean (since at least Archaean, 125 Feulner, 2012), the surface temperature would be stabilized by MEP to within low-tens degrees above the freezing point, which thus may resolve the FYSP.

With the global cloud known, Ou (2006, 2023b) then applies MEP to deduce its latitudinal tendency. To illustrate the basic physics, let us consider an ocean divided into warm/cold bands by a subtropical front, so its entropy production is simply the product of OHT and the differential temperature across the front. For a given thermal field, MEP then maximizes OHT, 130 which implies the same for the differential radiative forcing regulable by clouds. As such, the low cloud, which dominates the cloud albedo (Goldblatt & Zahnle, 2011), would be expelled to high latitudes, a deduction that is consistent with the observed vast stratus in high latitudes. With this tendency, we shall assume clouds as known, so the external forcing is the short-wave (SW) flux reaching the surface, which is subjected only to the land albedo.

Applying MEP to the atmosphere and ocean successively, Ou (2006, 2018) links the differential sea-surface temperature 135 (SST,  $T'$ ) to the differential forcing ( $q'$ ) via

$$T' = q'/\alpha, \quad (2)$$

where  $\alpha$  is the air-sea transfer coefficient augmented to include the latent heat. For an observational test, we set  $\alpha = 15 \text{ Wm}^{-2} \text{ }^\circ\text{C}^{-1}$  (Ou, 2018, his appendix B) and differential forcing of  $300 \text{ Wm}^{-2}$  (Peixoto & Oort, 1992, their figure 6.14), they would produce SST range of  $20 \text{ }^\circ\text{C}$ , comparable to the observed one (Kucera et al., 2005). As an additional test, the MEP- 140 deduced MOC has a simple expression  $\alpha A_{NA}(4\rho_o C_{p,o})^{-1}$  with  $A_{NA}$  being the area of the North Atlantic cold band (poleward of  $30^\circ \text{ N}$ ),  $\rho_o$ , the ocean density, and  $C_{p,o}$ , its specific heat. Surprisingly, this MOC does not even depend on differential forcing, whose effect apparently has been neutralized by the thermal response (2). For a North Atlantic width of 6000 km, MOC would be 17 Sv, which is commensurate with the observed one (Macdonald, 1998). This constitutes a stringent test since it involves no free parameters—unlike previous comparisons involving tunable diapycnal diffusivity (Dalan et al., 2005), hence 145 provides a strong support of MEP.

To recap, as a part of the present theory, prior derivations have determined the global temperature, its sensitivity to the global forcing (1), the linkage of the differential temperature and forcing (2), and latitudinal cloud—all have been tested against observation and can be regarded as known for the following derivations.

### 3 Box model

150 As a minimal representation of the observed ocean, we consider a box configuration as sketched in Fig. 2 where it is divided into tropical/polar bands of equal areas designated by numerals 1/2, and we assume for simplicity hemispheric symmetry so



only the hemispheric half is shown. As justified above, the external forcing is the SW flux reaching the surface ( $q_i^*$ ), which, after reflection by land, is absorbed by the ocean ( $q_i$ ) to differentiate the SST ( $T_i$ ) and drive the OHT, the latter composed partly of random eddies. The total land area  $A^*$  is known and its tropical portion  $A$  is the independent variable whose effect on the climate is to be examined.

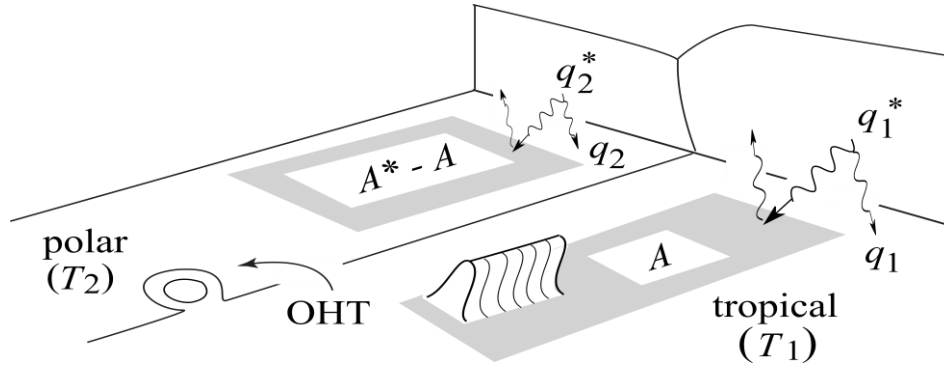


**Figure 2.** The model configuration in which the coupled ocean/atmosphere is divided into tropical/polar bands of equal areas designated by numerals 1/2. External forcing is the SW flux reaching the surface ( $q_i^*$ ), which, after reflection by land, is absorbed by the ocean ( $q_i$ ) to differentiate the SST ( $T_i$ ) and drive the OHT composed partly of random eddies. The total land area  $A^*$  is known and its tropical portion  $A$  is the independent variable whose effect is to be examined.

Because of the thermal inertia of the ocean, we neglect its seasonality (Kucera et al., 2005) so the radiative forcing  $q_i$  is the annual SW flux absorbed by the ocean. Although the SAT is seasonal, only the summer one is relevant in its control of the ablation hence the glacial margin. We assume the glacial margin to be zonal, so its marking temperature extends into the adjacent ocean, which moreover is assumed to be the same as the underlying SST in maintaining the radiative-convective equilibrium that defines the troposphere. In support of this assumption, the observed sea/air temperature difference in *summer* is no more than 2 °C globally (Peixoto & Oort, 1992, their figure 10.7, lower panel). We assume continents to have mountain ranges reaching above the snowline, so there is always glacier to seed its advance to the sea-level when temperature falls.

### 3.1 Radiative forcing

We first determine the radiative forcing as a function of the tropical land area (all areas are expressed in fractions of the global surface). With land reflectance  $r$ , the radiative forcings are

$$q_1 = q_1^*(1 - 2rA), \tag{3}$$

$$q_2 = q_2^*[1 - 2r(A^* - A)], \tag{4}$$

where the numerical factor 2 stems from band areas being 1/2 of the global surface. The global radiative forcing is

$$\bar{q} \equiv (q_1 + q_2)/2, \tag{5}$$

which thus varies with the tropical land area as

$$\delta\bar{q} = -r\Delta q^*\delta A, \tag{6}$$

where



$$\Delta q^* \equiv q_1^* - q_2^* \quad (7)$$

is the differential SW flux reaching the surface, an external parameter. For a crude estimate of the Proterozoic forcing, we take the current tropical/polar solar irradiance of  $400/100 \text{ Wm}^{-2}$  (Peixoto & Oort, 1992, their figure 6.13), reduce it by 10%, and apply cloud albedo of 0/0.5 (based on its deduced tendency in Sect. 2) to yield the external forcing of  $[q_1^*, q_2^*] = [360, 45] \text{ Wm}^{-2}$ . With no land plants in the Proterozoic, the land reflectance is that of a desert set to  $r = 0.5$  (Chandler & Sohl, 2000), and for a total land area set to 0.3, we plot in Fig. 3a radiative forcings against the tropical land area  $A$ . It is seen that as the land migrates into the tropics, it weakens the tropical forcing ( $q_1$ ) more than it strengthens the polar forcing ( $q_2$ ) because of the brighter tropical sun, resulting in a net reduction of global forcing ( $\bar{q}$ ) by  $47 \text{ Wm}^{-2}$ , which is quite substantial, amounting to doubling the Proterozoic dimming of the sun from the present.

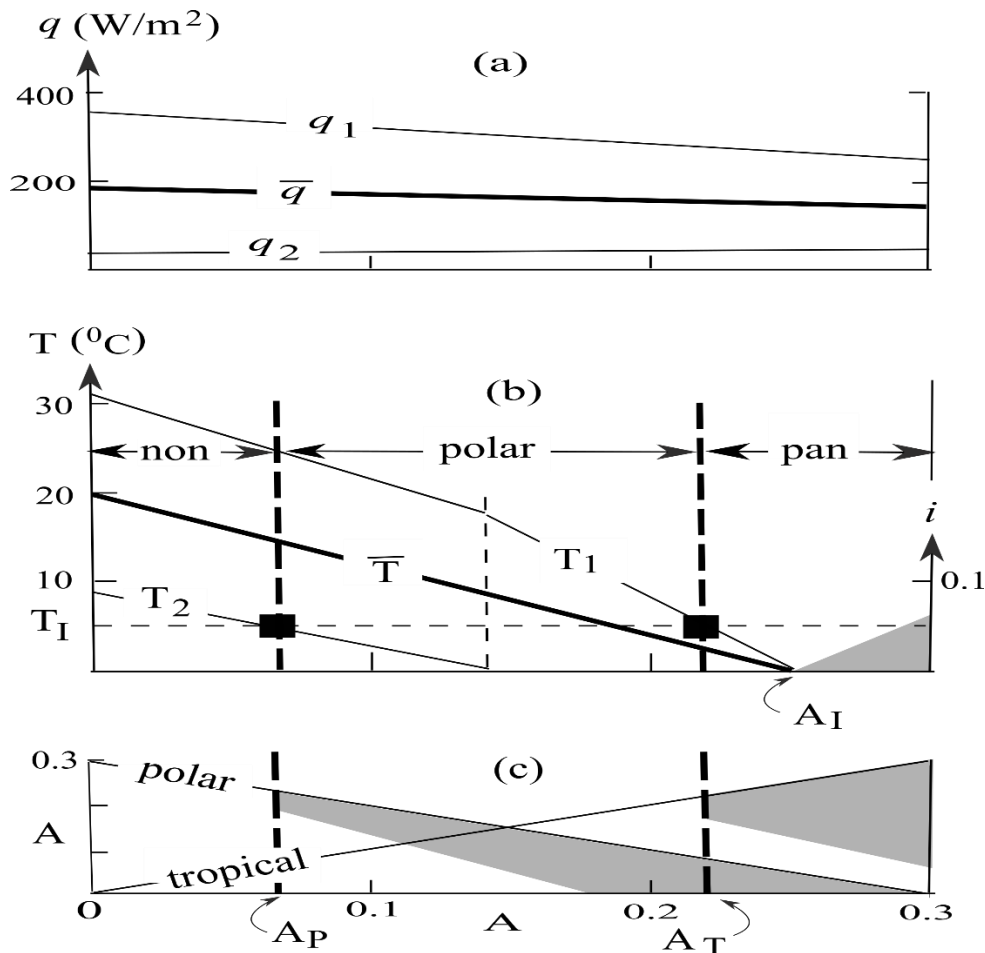


**Figure 3.** The radiative forcing (a), surface temperature (b) and land areas (c) plotted against the tropical land area  $A$ . Thick and thin lines are global-means and tropical/polar values subscripted 1/2, respectively. The temperature  $T_I$  marks the glacial margin whose intersections with tropical/polar temperatures (solid rectangles) divide non/polar/pan-glacial regimes with  $A_P/A_T$  being the thresholds for polar/tropical-glaciation and  $A_I$ , the onset threshold for perennial sea ice (shaded). Shades in (c) signify the glaciated area.





### 3.2 Sea-surface temperature

Given the radiative forcing and sensitivity (1), global temperature is specified by its maximum set to 20 °C (Scotese et al., 2021) and plotted in the thick solid line in Fig. 3b. For the chosen parameter values, the global temperature would cool to the  
195 freezing point with the tropical concentration of land but given the crudeness of the model and uncertain parameters, this scenario should be regarded as merely plausible, which, as seen later, is not required for the tropical glaciation.

Subjected to (2), we plot tropical/polar temperatures in thin lines. Since  $1/\alpha$  ( $= 0.07$ ) is much smaller than  $s$  ( $= 0.5$ ), one can see from (1) and (2) that both temperatures trend with the global cooling despite the increasing polar forcing. When the polar temperature reaches the freezing point (thin vertical dashed line), the tropical temperature would drop more sharply with  
200  $A$  until it is also cooled to the freezing point at  $A_T$ . As we shall see later, only when the tropical land area exceeds this threshold ( $A > A_T$ ) would there be perennial sea-ice, as shaded.

### 3.3 Land glaciation

With mountain ranges providing seeding for the sea-level land ice, the latter would advance equatorward by accumulation until halted by increasing ablation. Since ablation occurs only when the temperature is above the freezing point, so is the  
205 marking temperature of the glacial margin to counter the finite yearly accumulation. Through crude ice dynamics and mass balance, Ou (2023a) derives an expression for this marking temperature whose prognosed value  $T_I \approx 5$  °C is consistent with the present Greenland ice sheet (Oerlemans, 1991). This marking temperature is the horizontal dashed line of Fig. 3b whose intersections with tropical/polar temperatures (solid rectangles) then divide non/polar/pan-glacial regimes (thick vertical dashed lines) with  $A_P/A_T$  denoting the thresholds when ice would advance into the polar/tropical land, respectively.

For a box model, one obviously may not discern the glacial margin within each band or its longitudinal excursion on land, the above deduction nonetheless allows one to assess broad glacial extent, and to aid the visualization, we show in Fig. 3c tropical/polar land areas and their glaciated portions signified by shades. Increasing tropical land naturally shrinks the polar  
210 land, but the attendant cooling would expand the polar glaciation until it is limited by the available polar land, and when  $A_T$  is exceeded, there would be a strong glacial expansion into the tropical band—even when the polar glaciated surface shrinks to zero, as is the observed case (Evans & Raub, 2011). With vagaries of the tectonics that control the tropical land area  $A$  (that is, moving along the  $x$ -axis), one thus expects glacial advance/retreat on tectonic timescale, as observed (Rieu et al., 2007; Allen & Etienne, 2008), so should be the onset/termination of the tropical glaciation when  $A_T$  is crossed—not the millennial timescale governing the ice mass balance or the ice-albedo feedback (Ou, 2023a; Hyde et al., 2000).

Figure 3c points to a wide-spread misconception that increasing polar land always favors glaciation (Crowley & Baum,  
220 1993): As readily seen from the figure that this holds only if the polar land is already saturated by ice—for otherwise the accompanying warming would in fact shrink the glaciated surface to possibly vault it into the non-glacial regime, the latter thus may resolve the seeming puzzle of warm Cambrian despite polar positioning of Gondwana (Evans, 2003; Li et al., 2013). Since pan-glacial regime hinges on global cooling, tropical glaciations should be globally synchronous, as is the observed case





(Rooney et al., 2015; Hoffman et al., 2017), which incidentally invalidates the zipper-rift hypothesis of regional glaciation  
225 (Eyles & Januszczak, 2004). And then since the polar land is always glaciated in pan-glacial regime, it agrees with observation  
(Evans, 2003, his figure 7) but dispels the high-obliquity conjecture of Williams et al. (1998).

### 3.4 Perennial sea ice

The sea ice may form only when the polar water has cooled to the freezing point, and with the differential temperature fixed  
as such, MEP implies a maximized OHT. This leads immediately to vanishing perennial ice since any such ice would curb the  
230 ocean cooling hence OHT, contravening its maximization. One should note however that MEP operates on millennial timescale  
(Ou, 2018) so it does not preclude sea ice formation over shorter timescale, including the seasonal one. In fact, with the SST  
hovering around the freezing point, there is necessarily extensive winter ice, as seen during the last ice age, but tellingly the  
North Atlantic remains largely open in summer (de Vernal et al., 2005), a peculiarity that may be readily explained by MEP.  
Extending the above argument, we see that only when the tropical ocean is also cooled to the freezing point with the shutdown  
235 of OHT could there be perennial sea ice—even over the polar ocean. At this juncture  $A_I$ , the cooling flux at the ocean surface  
 $\bar{q}_o$  has reached its lower limit given by the radiative forcing  $\bar{q}_I$ ,

$$\bar{q}_o = \bar{q}_I, \quad (8)$$

so any further reduction of the radiative forcing (that is,  $\bar{q} < \bar{q}_I$ ) must induce sea-ice cover ( $i$ ) to maintain the ocean heat  
balance

$$240 \quad \bar{q}_o (1 - i) = \bar{q} - iq_2^*, \quad (9)$$

where the last term represents the positive feedback between sea ice and the radiative forcing (assuming sea ice remains in the  
polar band, to be checked later). Substituting (8) into (9), we obtain

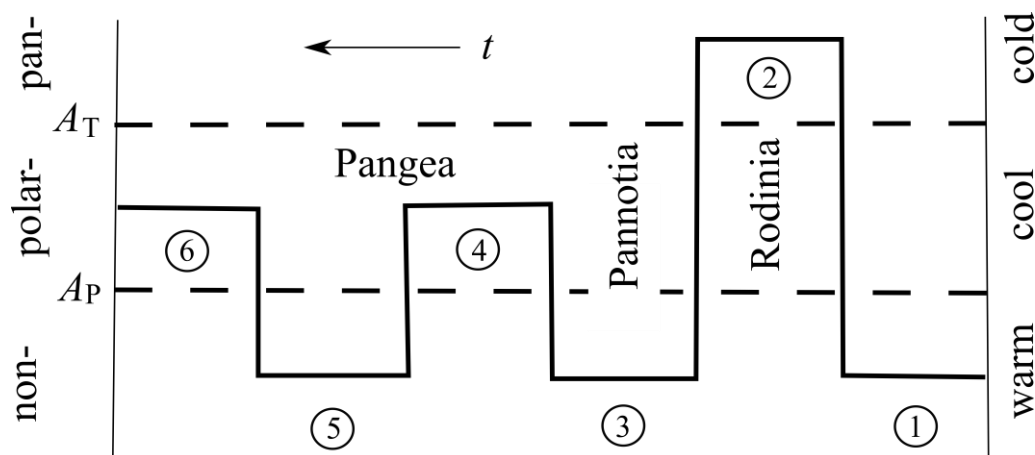
$$i = \frac{1 - \bar{q}/\bar{q}_I}{1 - q_2^*/\bar{q}_I}, \quad (10)$$

the sea ice thus is fully specified by radiative forcing, as shaded in Fig. 3b. It increases linearly with decreasing  $\bar{q}$  and attains  
245 a maximum of about 6% of the global surface, a deduction that is consistent with the observation that there is little sea ice for  
all glacio-epochs (Eyles, 2008). Equation (10) also shows the importance of positive ice-albedo feedback without which the  
sea ice cover would be halved.

It is seen therefore that even when the global ocean is cooled to the freezing point, the perennial ice remains confined to  
high latitudes, so despite crudeness of our box model, the tropical ocean for all practical purposes should remain open to  
250 maintain active hydrological cycle, as observed but contrary to iceball earth.

## 4 Glacio-epochs chronology

We have identified non/polar/pan-glacial regimes controlled by the tropical appropriation of land and based on the observed  
paleogeography (Eyles, 2008; Bradley, 2011; Li et al., 2013; Nance et al., 2014), we offer the following interpretation of the  
glacio-epochs aided by the numbered stages shown in Fig. 4 (time moves to the left).



255

**Figure 4.** The model interpretation of glacio-epochs based on observed paleogeography (time moves to left), aided by numbered stages. Dashed lines are tropical-land thresholds that divide non/polar/pan-glacial regimes.

Stage 1 represents the bulk of Proterozoic when there are no supercontinents to concentrate the tropical land and, with the fainter sun being moderated by less cloud (Sect. 2), the climate is too warm for glaciation. With our hypothesis of glacio-epochs in equilibrium with paleogeography, there is thus no significant puzzle for a billion-year long glacial lull (Pierrehumbert et al., 2011).

Stage 2 represents the tropical tenure of supercontinents, which would block the brighter tropical sun to cause the tropical glaciation. This pan-glacial state seems to occur to all Precambrian supercontinents (named glaciations indicated)—definitely to Ur (Pongola), Kenorland (Huronian), and Rodinia (Sturtian, Marinoan, Gaskiers), and possibly to Columbia (nameless) (Eyles, 2008; Young, 2013; Williams et al., 2016). Although glacial deposits are mostly found in rift basins, it could reflect preservation bias (Eyles, 2008) since weathering is also elevated during assembly of supercontinents (Maruyama & Santosh, 2008; Macdonald et al., 2019) and indeed Huronian glacial deposits precede the breakup of Kenorland (Young, 2013). Bypassing the questionable role of  $p\text{CO}_2$  (Kerrick & Caldeira, 1999, see also Sect. 1) and uncertain paleogeography, we can only ascribe pan-glacial regime to the tropical cluster of landmasses not their detailed evolution. The vagaries of such evolution on tectonic timescale may accommodate disparate durations of Sturtian/Marinoan/Gaskiers (50/5/1 million years) (Li et al., 2013; Stern & Miller, 2021), which are difficult to bridge by iceball earth because of the minimum time needed to build up  $p\text{CO}_2$  for deglaciation (Hoffman et al., 1998; Godd ris et al., 2021).

Stage 3 marks the breakup of Rodinia, which reassembles as Pannotia near the south pole during early Paleozoic (Li et al., 2013; Murphy et al., 2021). The lack of tropical land has propelled the climate to non-glacial regime as seen in the warm Cambrian (Hearing et al., 2018, see also Sect. 3.3). The warmth is temporarily reversed in late Ordovician when Laurentia and Baltica rift away from Gondwana and enter the tropics (Marcilly et al., 2022), causing the Andean-Saharan glaciation, which thus need not involve volcanic eruption or bolide collision (Scotese et al., 2021).

Stage 4 represents the assembly of Pangea when Laurentia reattaches Gondwana to extend from pole-to-pole (Nance et al., 2014). Although there is more tropical land than Pannotia, the sizable polar land hence the associated warmth only allows



280 polar-glaciation (Karoo) lasting about 100 million years (Eyles, 2008). Based on our model, it is thus the smaller tropical land  
of Pangea in comparison with Precambrian supercontinents that distinguishes Phanerozoic and Precambrian glacio-epochs  
(Evans, 2000), which otherwise are subjected to the same physics in adherence to the uniformitarianism (Etienne et al., 2007),  
again there is no need to invoke extraneous and unsupported physics of iceball earth.

Stage 5 represents the breakup of Pangea that propels land into high northern latitudes (Eyles, 2008), the ensuing warmth  
285 may account for the non-glacial interval spanning Mesozoic and early Cenozoic. Together with Stage 3, they correspond to  
the classical double humps (Fischer, 1982). This warming reverses in Eocene when climate begins to cool (Eyles, 2008), which  
has been attributed to the uplift of Himalayas and enhanced weathering (Raymo & Ruddiman, 1992), whose efficacy however  
has been questioned (Kerrick & Caldeira, 1999). Adhering to the paleogeographic control, it is also possible to ascribe this  
cooling to the polar centering of Antarctica accompanied by opening of the Drake Passage (Eyles, 2008), which would have  
290 deprived the Antarctic interior from the ocean heat, causing it to icing over accompanied by global cooling, a conjecture that  
is examined in a forthcoming paper.

Stage 6 represents the current polar-glacial regime (Quaternary) (Young, 2013). The contiguous northern land extending  
into the subtropics allows glacial advance/retreat in response to the orbital forcing (Milankovitch, 1941). Applying MEP in a  
box model, Ou (2023a) shows that Cenozoic cooling may account for the mid-Pleistocene transition from obliquity- to  
295 eccentricity-dominated glacial cycles, which thus can be integrated into the deep-time framework presented here. The orbital-  
period glacial cycles however should be distinguished from aperiodic glacio-epochs of tectonic timescale (Allen & Etienne,  
2008).

## 5 Conclusion

An extreme scenario was previously proposed to explain Cryogenian tropical glaciations, which invokes runaway ice-albedo  
300 feedback leading to an iceball earth. In addition to its conflict with sedimentary data showing an open ocean, we point out  
flawed physics of the runaway scenario and deficient closure of numerical models in addressing the problem. As an  
alternative, we advance the uniformitarian view that the thermodynamic closure of the system must accommodate both FYSP  
and tropical glaciation, and that the two should be distinguished only by external conditions.

For the thermodynamic closure, we posit that, because of the inherently turbulent nature of the planetary fluids, the generic  
305 climate state is a macroscopic manifestation of a NT system hence characterized by maximum entropy production (MEP), a  
generalized second law. And for discernible external conditions, we posit that Precambrian supercontinents may block the  
brighter tropical sun to cause tropical glaciation. To test this hypothesis in a most transparent manner, we formulate a minimal  
tropical/polar box model to examine the effect of differential land partition on the climate and glacial regimes. As a part of the  
present theory, prior applications of MEP by this author have determined certain thermal properties and together with new  
310 findings, they are summarized below.



- Applying MEP in a global-mean aquaplanet model, Ou (2001) shows that global cloud would self-adjust to render habitable temperature constrained by intrinsic water properties (Clausius–Clapeyron relation), thereby resolving the FYSP. The closure allows the determination of the global temperature and its sensitivity to the radiative forcing.
- Applying MEP to a latitudinal model, Ou (2006) shows that low clouds, which dominate the cloud albedo, are expelled to high latitudes, thereby maximizing the differential forcing, the latter in turn specifies the differential temperature.
- Applying MEP and foregoing constraints in a box model, we produce a regime diagram showing cooling tropical/polar temperatures when increasing tropical land would block the brighter tropical sun. Even when the global ocean is cooled to the freezing point, the perennial sea ice remains confined to high latitudes, thwarting therefore the runaway ice-albedo feedback.
- The glacial margin is marked by above-freezing temperature to counter the yearly accumulation, whose crossing by tropical/polar temperatures would divide non/polar/pan-glacial regimes, the last being characterized by tropical glaciation abutting an open ocean.
- Given the observed paleogeography, the model may provide a unified account of glacio-epochs through Earth’s history. Precambrian and Phanerozoic glacio-epochs differ only by tropical appropriation of the land in its blockage of the brighter tropical sun.

In conclusion, through a minimal box model subjected to MEP, our theory provides a unified account of FYSP, Precambrian tropical glaciations, and glacio-epochs through Earth’s history—all are differentiated by paleogeography varying on tectonic timescale, in support of the uniformitarian principle.

**Data availability:** No proprietary data are used.

**Competing interests:** This author declares no conflicting interest relevant to this study.

**Acknowledgments:** None

## References

- Allen PA, Etienne JL (2008) Sedimentary challenge to Snowball Earth. *Nat Geosci* 1:817-25 <https://doi.org/10.1038/ngeo355>
- Bendtsen J (2002) Climate sensitivity to changes in solar insolation in a simple coupled climate model. *Clim Dyn* 18:595–609 <https://doi.org/10.1007/s00382-001-0198-4>
- Berner RA, Caldeira K (1997) The need for mass balance and feedback in the geochemical carbon cycle. *Geol* 25(10):955-6 [https://doi.org/10.1130/0091-7613\(1997\)025<0955:tnfmba>2.3.co;2](https://doi.org/10.1130/0091-7613(1997)025<0955:tnfmba>2.3.co;2)
- Bice KL, Scotese CR, Seidov D, Barron EJ (2000) Quantifying the role of geographic change in Cenozoic ocean heat transport using uncoupled atmosphere and ocean models. *Palaeogeogr Palaeoclimatol Palaeoecol* 161:295–310 [https://doi.org/10.1016/s0031-0182\(00\)00072-9](https://doi.org/10.1016/s0031-0182(00)00072-9)
- Boucot AJ, Gray J (2001) A critique of Phanerozoic climatic models involving changes in the CO<sub>2</sub> content of the atmosphere. *Earth Sci Rev* 56(1-4):1-59 [https://doi.org/10.1016/s0012-8252\(01\)00066-6](https://doi.org/10.1016/s0012-8252(01)00066-6)
- Bradley DC (2011) Secular trends in the geologic record and the supercontinent cycle. *Earth Sci Rev* 108(1-2):16-33 <https://doi.org/10.1016/j.earscirev.2011.05.003>



- 345 Brady PV, Carroll SA (1994) Direct effects of CO<sub>2</sub> and temperature on silicate weathering: possible implications for climate control. *Geochim Cosmochim Acta* 58:1843–56 [https://doi.org/10.1016/0016-7037\(94\)90543-6](https://doi.org/10.1016/0016-7037(94)90543-6)
- Braun C, Hörner J, Voigt A, Pinto JG (2022) Ice-free tropical waterbelt for Snowball Earth events questioned by uncertain clouds. *Nat Geosci* (6):489–93 <https://doi.org/10.1038/s41561-022-00950-1>
- Bruers S (2007) A discussion on maximum entropy production and information theory. *J Phys A: Math Theor* 40(27):7441–  
350 50 <https://doi.org/10.1088/1751-8113/40/27/003>
- Budyko MI (1969) The effect of solar radiation variations on the climate of the Earth. *Tellus* 21(5):611–9  
<https://doi.org/10.1111/j.2153-3490.1969.tb00466.x>
- Chandler MA, Sohl LE (2000) Climate forcings and the initiation of low-latitude ice sheets during the Neoproterozoic Varanger glacial interval. *J Geophys Res* 105(D16):20737–56 <https://doi.org/10.1029/2000jd900221>
- 355 Christie-Blick N, Sohl LE, Kennedy MJ (1999) Considering a Neoproterozoic snowball earth. *Science* 284(5417):1087  
<https://doi.org/10.1126/science.284.5417.1087a>
- Chumakov NM, Elston DP (1989) The paradox of Late Proterozoic glaciations at low latitudes. *Episodes* 12(2):115–20  
<https://doi.org/10.18814/epiugs/1989/v12i2/015>
- Chumakov NM (2008) A problem of total glaciations on the Earth in the Late Precambrian. *Stratigr Geol Correl* 16(2):107–19  
360 <https://doi.org/10.1134/s0869593808020019>
- Colin de Verdière A (1988) Buoyancy driven planetary flows. *J Mar Res* 46(2):215–65  
<https://doi.org/10.1357/002224088785113667>
- Condon DJ, Prave AR, Benn DI (2002) Neoproterozoic glacial-rainout intervals: observations and implications. *Geol* 30(1):35–  
8 [https://doi.org/10.1130/0091-7613\(2002\)030<0035:ngrioa>2.0.co;2](https://doi.org/10.1130/0091-7613(2002)030<0035:ngrioa>2.0.co;2)
- 365 Crooks GE (1999) Entropy production fluctuation theorem and the nonequilibrium work relation for free energy differences. *Phys Rev E* 60(3):2721–6 <https://doi.org/10.1103/physreve.60.2721>
- Crowley TJ, Baum SK (1993) Effect of decreased solar luminosity on late Precambrian ice extent. *J Geophys Res* 98(D9):16723–32 <https://doi.org/10.1029/93jd01415>
- Crowley TJ, North GR (1991) *Paleoclimatology*. Oxford University Press, 339 pp.
- 370 Dalan F, Stone PH, Kamenkovich IV, Scott JR (2005) Sensitivity of the ocean’s climate to diapycnal diffusivity in an EMIC. Part I: Equilibrium state. *J Clim* 18(13):2460–81 <https://doi.org/10.1175/jcli3411.1>
- de Vernal A, Eynaud F, Henry M, Hillaire-Marcel C, Londeix L, Mangin S, Matthiessen J, Marret F, Radi T, Rochon A, Solignac S, Turon JL (2005) Reconstruction of sea surface conditions at middle to high latitudes of the Northern Hemisphere during the Last Glacial Maximum (LGM) based on dinoflagellate cyst assemblages. *Quat Sci Rev* (24):897–  
375 924 <https://doi.org/10.1016/j.quascirev.2004.06.014>
- Dewar RC, Lineweaver CH, Niven RK, Regenauer-Lieb K (2014) Beyond the second law: an overview. In *Beyond the Second Law* (pp. 3–27). Springer Berlin Heidelberg. [https://doi.org/10.1007/978-3-642-40154-1\\_1](https://doi.org/10.1007/978-3-642-40154-1_1)



- Donnadieu Y, Ramstein G, Fluteau F, Roche D, Ganopolski A (2004) The impact of atmospheric and oceanic heat transports on the sea-ice-albedo instability during the Neoproterozoic. *Clim Dyn* 22:293–306. <https://doi.org/10.1007/s00382-003-0378-5>  
380
- Etienne JL, Allen PA, Rieu R, Le Guerroué E (2007) Neoproterozoic glaciated basins: a critical review of the Snowball Earth hypothesis by comparison with Phanerozoic glaciations. *Glacial Sedimentary Processes and Products*, Eds Hambrey MJ, Christoffersen P, Glasser NF, Hubbard B, 343-99 <https://doi.org/10.1002/9781444304435.ch19>
- Evans DAD (2003) A fundamental Precambrian–Phanerozoic shift in earth's glacial style? *Tectonophysics* 375:353–85  
385 [https://doi.org/10.1016/s0040-1951\(03\)00345-7](https://doi.org/10.1016/s0040-1951(03)00345-7)
- Evans D, Raub T (2011) Neoproterozoic glacial palaeolatitudes: A global update. *Geol Soc London Mem* 36(1):93–112  
<https://doi.org/10.1144/m36.7>
- Evans DJ, Searle DJ (2002) The fluctuation theorem. *Adv Phys* 51:1529 <https://doi.org/10.1080/00018730210155133>
- Eyles N (2008) Glacio-epochs and the supercontinent cycle after~ 3.0 Ga: tectonic boundary conditions for glaciation. *Palaeogeogr Palaeoclimatol Palaeoecol* 258(1-2):89-129 <https://doi.org/10.1016/j.palaeo.2007.09.021>  
390
- Eyles N, Januszczak N (2004) ‘Zipper-rift’: a tectonic model for Neoproterozoic glaciations during the breakup of Rodinia after 750 Ma. *Earth Sci Rev* (65):1– 73 [https://doi.org/10.1016/s0012-8252\(03\)00080-1](https://doi.org/10.1016/s0012-8252(03)00080-1)
- Fairchild IJ, Kennedy MJ (2007) Neoproterozoic glaciation in the Earth System. *J Geol Soc* 164(5):895-921  
<https://doi.org/10.1144/0016-76492006-191>
- 395 Feulner G (2012) The faint young Sun problem. *Rev Geophys* 50, RG2006 <https://doi.org/10.1029/2011RG000375>
- Fischer AG (1982) Long-term climate oscillations recorded in stratigraphy. *Climate in Earth history*:97-104
- Fraedrich K, Lunkeit F (2008) Diagnosing the entropy budget of a climate model. *Tellus A* 60(5):921-31  
<https://doi.org/10.1111/j.1600-0870.2008.00338.x>
- Godderis Y, Donnadieu Y (2019) A sink-or a source-driven carbon cycle at the geological timescale? Relative importance of palaeogeography versus solid Earth degassing rate in the Phanerozoic climatic evolution. *Geol Mag* 156(2):355-65  
400 <https://doi.org/10.1017/s0016756817001054>
- Goldblatt C, Zahnle KJ (2011) Clouds and the faint young Sun paradox. *Clim Past* 7(1):203–20 <https://doi.org/10.5194/cp-7-203-201>
- Harland WB (2007) Origins and assessment of snowball Earth hypotheses. *Geol Mag* 144(4):633-42  
405 <https://doi.org/10.1017/s0016756807003391>
- Hearing TW, Harvey TH, Williams M, Leng MJ, Lamb AL, Wilby PR, Gabbott SE, Pohl A, Donnadieu Y (2018) An early Cambrian greenhouse climate. *Sci Adv* (5):eaar5690 <https://doi.org/10.1126/sciadv.aar5690>
- Hoffman PF, Kaufman AJ, Halverson GP, Schrag DP (1998) A Neoproterozoic snowball earth. *Science* 281(5381):1342-6  
<https://doi.org/10.1126/science.281.5381.1342>
- 410 Hoffman PF, Abbot DS, Ashkenazy Y, Benn DI, Brocks JJ, Cohen PA, Cox GM, Creveling JR, Donnadieu Y, Erwin DH, Fairchild IJ, Ferreira D, Goodman JC, Halverson GP, Jansen MF, Le Hir G, Love GD, Macdonald FA, Maloof AC, Partin





- CA, Ramstein G, Rose BEJ, Rose CV, Sadler PM, Tziperman E, Voigt A, Warren SG (2017) Snowball Earth climate dynamics and Cryogenian geology–geobiology. *Sci Adv* 3, e1600983:1–43 <https://doi.org/10.1126/sciadv.1600983>
- 415 Hogg AM, Gayen B (2020) Ocean gyres driven by surface buoyancy forcing. *Geophys Res Lett* 47:e2020GL088539 <https://doi.org/10.1002/essoar.10503133.1>
- Hörner J, Voigt A, Braun C (2022) Snowball Earth initiation and the thermodynamics of sea ice. *J Adv Model Earth Syst* 14(8):e2021MS002734 <https://doi.org/10.5194/egusphere-egu22-5167>
- Hyde WT, Crowley TJ, Baum SK, Peltier WR (2000) Neoproterozoic ‘snowball Earth’ simulations with a coupled climate/ice-sheet model. *Nature* 405(6785):425–9 <https://doi.org/10.1038/35013005>
- 420 Jenkins GS, Smith SR (1999) GCM simulations of snowball Earth conditions during the late Proterozoic. *Geophys Res Lett* 26:2263–6 <https://doi.org/10.1029/1999gl1900538>
- Jiang G, Kennedy MJ, Christie-Blick N (2003) Stable isotopic evidence for methane seeps in Neoproterozoic postglacial cap carbonates. *Nature* 426:822–6 <https://doi.org/10.1038/nature02201>
- Kasting JF (1993) Earth’s early atmosphere. *Science* 259:920–6 <https://doi.org/10.1126/science.11536547>
- 425 Kennedy MJ, Christie-Blick N, Sohl LE (2001) Are Proterozoic cap carbonates and isotopic excursions a record of gas hydrate destabilization following Earth’s coldest intervals? *Geol* 29:443–6 [https://doi.org/10.1130/0091-7613\(2001\)029<0443:apccai>2.0.co;2](https://doi.org/10.1130/0091-7613(2001)029<0443:apccai>2.0.co;2)
- Kerrick DM, Caldeira K (1999) Was the Himalayan orogen a climatically significant coupled source and sink for atmospheric CO<sub>2</sub> during the Cenozoic? *Earth Planet Sci Lett* 173:195–203 [https://doi.org/10.1016/s0012-821x\(99\)00229-0](https://doi.org/10.1016/s0012-821x(99)00229-0)
- 430 Kilner B, Niocaill C, Brasier M (2005) Low-latitude glaciation in the Neoproterozoic of Oman. *Geol* 33(5):413–6 <https://doi.org/10.1130/g21227.1>
- Kirschvink JL (1992) Late Proterozoic low-latitude global glaciation: the snowball Earth. In Schopf JW, Klein C (eds) *The Proterozoic Biosphere: A Multidisciplinary Study*. Cambridge University Press. pp. 51–2
- Kleidon A, Fraedrich K, Kunz T, Lunkeit F (2003) The atmospheric circulation and states of maximum entropy production. *Geophys Res Lett* 30(23):2223 <https://doi.org/10.1029/2003gl018363>
- 435 Kleidon A (2009) Non-equilibrium thermodynamics and maximum entropy production in the Earth system: applications and implications. *Naturwissenschaften* 96:653–77 <https://doi.org/10.1007/s00114-009-0509-x>
- Kleidon A, Zehe E, Ehret U, Scherer U (2014) Earth system dynamics beyond the second law: Maximum power limits, dissipative structures, and planetary interactions. In *Beyond the Second Law: Entropy Production and Non-equilibrium Systems*, Springer Berlin Heidelberg, 163–82 [https://doi.org/10.1007/978-3-642-40154-1\\_8](https://doi.org/10.1007/978-3-642-40154-1_8)
- 440 Kucera M, Weinelt M, Kiefer T, Pflaumann U, Hayes A, Weinelt M, Chen MT, Mix AC, Barrows TT, Cortijo E, Duprat J (2005) Reconstruction of sea-surface temperatures from assemblages of planktonic foraminifera: multi-technique approach based on geographically constrained calibration data sets and its application to glacial Atlantic and Pacific Oceans. *Quat Sci Rev* 24(7–9):951–98 <https://doi.org/10.1016/j.quascirev.2004.07.014>





- 445 Kunz T, Fraedrich K, Kirk E (2008) Optimisation of simplified GCMs using circulation indices and maximum entropy production. *Clim Dyn* 30(7):803-13 <https://doi.org/10.1007/s00382-007-0325-y>
- Leather J, Allen P, Brasier M, Cozzi A (2002) Neoproterozoic snowball Earth under scrutiny: Evidence from the Fiq glaciation of Oman. *Geol* 30:891-4 [https://doi.org/10.1130/0091-7613\(2002\)030<0891:nseuse>2.0.co;2](https://doi.org/10.1130/0091-7613(2002)030<0891:nseuse>2.0.co;2)
- Le Guerrouè E, Allen PA, Cozzi A (2006) Chemostratigraphic and sedimentological framework of the largest negative carbon isotopic excursion in Earth history: The Neoproterozoic Shuram formation (Nafun Group, Oman). *Precambr Res* 146:68-92 <https://doi.org/10.1016/j.precamres.2006.01.007>
- 450 Li ZX, Evans DAD, Halverson GP (2013) Neoproterozoic glaciations in a revised global palaeogeography from the breakup of Rodinia to the assembly of Gondwanaland. *Sediment Geol* 294:219-32 <https://doi.org/10.1016/j.sedgeo.2013.05.016>
- Liu T, Ou HW, Liu X, Chen D (2022) On the role of eddy mixing in the subtropical ocean circulation. *Front Mar Sci* 9:832992 <https://doi.org/10.1002/essoar.10506284.1>
- 455 Lorenz RD, Lunine JI, Withers PG, McKay CP (2001) Titan, Mars and Earth: Entropy production by latitudinal heat transport. *Geophys Res Lett* 28(3):415-8 <https://doi.org/10.1029/2000gl012336>
- Lozier MS (2010) Deconstructing the conveyor belt. *Science* 328(5985):1507-11 <http://doi.org/10.1126/science.1189250>
- Lucarini V, Fraedrich K, Ragone F (2011) New results on the thermodynamic properties of the climate system. *J Atmos Sci* 68(10):2438-58 <https://doi.org/10.1175/2011jas3713>
- 460 Macdonald AM (1998) The global ocean circulation: A hydrographic estimate and regional analysis. *Prog Oceanogr* 41(3):281-382 [https://doi.org/10.1016/s0079-6611\(98\)00020-2](https://doi.org/10.1016/s0079-6611(98)00020-2)
- Macdonald FA, Swanson-Hysell NL, Park Y, Lisiecki L, Jagoutz O (2019) Arc-continent collisions in the tropics set Earth's climate state. *Science* 364(6436):181-4 <https://doi.org/10.1126/science.aav5300>
- 465 Marcilly CM, Maffre P, Le Hir G, Pohl A, Fluteau F, Godd ris Y, Donnadi u Y, Heimdal TH, Torsvik TH (2022) Understanding the early Paleozoic carbon cycle balance and climate change from modelling. *Earth Planet Sci Lett* 594:117717 <https://doi.org/10.1016/j.epsl.2022.117717>
- Martyushev LM, Seleznev VD (2006) Maximum entropy production principle in physics, chemistry and biology. *Phys Rep* 426(1):1-45 <https://doi.org/10.1016/j.physrep.2005.12.001>
- 470 Maruyama S, Santosh M (2008) Models on Snowball Earth and Cambrian explosion: a synopsis. *Gondwana Res* 14:22-32 <https://doi.org/10.1016/j.gr.2008.01.004>
- Milankovitch M (1941) Canon of insolation and the ice-age problem. R Serb Acad Spec Publ 132 (Translated from German, Israel Program for Scientific Translations) Jerusalem, 1969
- Murphy JB, Strachan RA, Quesada C (2021) Pannotia to Pangaea: Neoproterozoic and Paleozoic Orogenic cycles in the Circum-Atlantic region: a celebration of the career of Damian Nance. *Geol Soc, London, Special Publications* 503(1):1 <https://doi.org/10.1144/sp503>
- 475 Nance RD, Murphy JB, Santosh M (2014) The supercontinent cycle: a retrospective essay. *Gondwana Res* 25(1):4-29 <https://doi.org/10.1016/j.gr.2012.12.026>



- Oerlemans J (1991) The mass balance of the Greenland ice sheet: sensitivity to climate change as revealed by energy-balance  
480 modelling. *Holocene* 1(1):40-8 <https://doi.org/10.1177/095968369100100106>
- Ou HW (2001) Possible bounds on the earth's surface temperature: from the perspective of a conceptual global-mean model.  
J Clim 14:2976–88 [https://doi.org/10.1175/1520-0442\(2001\)014<2976:pbotes>2.0.co;2](https://doi.org/10.1175/1520-0442(2001)014<2976:pbotes>2.0.co;2)
- Ou HW (2006) Meridional thermal field of a coupled ocean-atmosphere system: a conceptual model. *Tellus* 58A:404-15  
<https://doi.org/10.1111/j.1600-0870.2006.00174.x>
- 485 Ou HW (2018) Thermohaline circulation: a missing equation and its climate change implications. *Clim Dyn* 50:641-53  
<https://doi.org/10.1007/s00382-017-3632-y>
- Ou HW (2023a) A theory of orbital-forced glacial cycles: resolving Pleistocene puzzles. *J Mar Sci Eng* 11(3):564  
<https://doi.org/10.3390/jmse11030564>
- Ou HW (2023b) Hemispheric symmetry of planetary albedo: a corollary of nonequilibrium thermodynamics. *Atmosphere*  
490 14:1243 <https://doi.org/10.3390/atmos14081243>
- Ozawa H, Ohmura A, Lorenz RD, Pujol T (2003) The second law of thermodynamics and the global climate system: A review  
of the maximum entropy production principle. *Rev Geophys* 41:4/10182003 <https://doi.org/10.1029/2002rg000113>
- Paltridge G (1975) Global dynamics and climate—a system of minimum entropy exchange. *Q J R Meteorol Soc* (101):475–84  
<https://doi.org/10.1002/qj.49710142906>
- 495 Pauluis O, Held IM (2002) Entropy budget of an atmosphere in radiative–convective equilibrium. Part I: Maximum work and  
frictional dissipation. *J Atm Sci* 59(2):125-39 [https://doi.org/10.1175/1520-0469\(2002\)059<0125:eboaai>2.0.co;2](https://doi.org/10.1175/1520-0469(2002)059<0125:eboaai>2.0.co;2)
- Peixoto JP, Oort AH (1992) *Physics of Climate*. Amer Inst Phys, New York
- Pierrehumbert RT, Abbot DS, Voigt A, Koll D (2011) Climate of the Neoproterozoic. *Annu Rev Earth Planet Sci* 39:417–60  
<https://doi.org/10.1146/annurev-earth-040809-152447>
- 500 Pollard D, Kasting JF (2004) Climate-ice sheet simulations of Neoproterozoic glaciation before and after collapse to Snowball  
Earth. In *The Extreme Proterozoic: Geology, Geochemistry, and Climate*, *Geophys Monogr Ser* (146) edited by Jenkins  
G, McMenamin M, McKay C, Sohl L, pp. 91– 105, AGU, Washington DC <https://doi.org/10.1029/146gm09:91-105>.
- Poulsen CJ, Pierrehumbert RT, Jacob RL (2001) Impact of ocean dynamics on the simulation of the Neoproterozoic “snowball  
Earth”. *Geophys Res Lett* 28(8):1575-8 <https://doi.org/10.1029/2000gl012058>
- 505 Rahmstorf S, Crucifix M, Ganopolski A, Goosse M, Kamenkovich I, Knutti R, Lohmann G, Marsh R, Mysak LA, Wang Z,  
Weaver AJ (2005) Thermohaline circulation hysteresis: A model intercomparison. *Geophys Res Lett* 32(23) L23605,  
[doi:10.1029/2005GL023655](https://doi.org/10.1029/2005GL023655)
- Raymo ME, Ruddiman WF (1992) Tectonic forcing of late Cenozoic climate. *Nature* 359(6391):117-22  
<https://doi.org/10.1038/359117a0>
- 510 Rieu R, Allen PA, Plötze M, Pettke T (2007) Climatic cycles during a Neoproterozoic “snow-ball” glacial epoch. *Geol*  
35(4):299-302 <https://doi.org/10.1130/g23400a.1>



- Rooney AD, Strauss JV, Brandon AD & Macdonald FA (2015) A Cryogenian chronology: Two long-lasting synchronous Neoproterozoic glaciations. *Geol* 43:459–62 <https://doi.org/10.1130/g36511.1>
- 515 Sansjofre P, Ader M, Trindade RI, Elie M, Lyons J, Cartigny P, Nogueira AC (2011) A carbon isotope challenge to the snowball Earth. *Nature* 478(7367):93–6 <https://doi.org/10.1038/nature10499>
- Scotese CR, Song H, Mills BJ, van der Meer DG (2021) Phanerozoic paleotemperatures: The earth’s changing climate during the last 540 million years. *Earth Sci Rev* 215:103503 <https://doi.org/10.1016/j.earscirev.2021.103503>
- Sheldon ND, Mitchell RL, Dzombak RM. *Reconstructing Precambrian pCO<sub>2</sub> and pO<sub>2</sub> using paleosols* (2021) Cambridge University Press <https://doi.org/10.1017/9781108870962>
- 520 Shimokawa S, Ozawa H (2002) On the thermodynamics of the oceanic general circulation: Irreversible transition to a state with higher rate of entropy production. *Q J R Meteorolog Soc* 128(584):2115–28 <https://doi.org/10.1256/003590002320603566>
- Sohl LE, Christie-Blick N, Kent DV (1999) Paleomagnetic polarity reversals in Marinoan (ca. 600 Ma) glacial deposits of Australia: implications for the duration of low-latitude glaciation in Neoproterozoic time. *Geol Soc Am Bull* 111(8):1120–39 [https://doi.org/10.1130/0016-7606\(1999\)111<1120:pprime>2.3.co;2](https://doi.org/10.1130/0016-7606(1999)111<1120:pprime>2.3.co;2)
- 525 Stern RJ, Miller NR (2021) Neoproterozoic Glaciation—Snowball Earth Hypothesis. *Encyclopedia Geol* (Second Edition):546–56 <https://doi.org/10.1016/b978-0-12-409548-9.12107-4>
- Voigt A, Abbot DS, Pierrehumbert RT, Marotzke J (2011) Initiation of a Marinoan Snowball Earth in a state-of-the-art atmosphere-ocean general circulation model. *Clim Past* 7:249–63 <https://doi.org/10.5194/cp-7-249-2011>
- 530 Walker JCG, Hays PB, Kasting JF (1981) A negative feedback mechanism for the long-term stabilization of Earth’s surface temperature. *J Geophys Res* 86:9776–82 <https://doi.org/10.1029/jc086ic10p09776>
- Wang GM, Sevick EM, Mittag E, Searles DJ, Evans DJ (2002) Experimental demonstration of violations of the Second Law of Thermodynamics for small systems and short time scales. *Phys Rev Lett* 89(5):050601/1–050601/4
- Williams DM, Kasting JF, Frakes LA (1998) Low-latitude glaciation and rapid changes in the Earth’s obliquity explained by obliquity–oblateness feedback. *Nature* 396(6710):453–5 <https://doi.org/10.1038/24845>
- 535 Williams GE, Schmidt PW, Young GM (2016) Strongly seasonal Proterozoic glacial climate in low palaeolatitudes: Radically different climate system on the pre-Ediacaran Earth. *Geosci Front* 7(4):555–71 <https://doi.org/10.1016/j.gsf.2016.01.005>
- Yang J, Peltier W, Hu Y (2012) The initiation of modern “soft Snowball” and “hard Snowball” climates in CCSM3. Part I: The influence of solar luminosity, CO<sub>2</sub> concentration and the sea-ice/snow albedo parameterization. *J Clim* 25:2711–36 <https://doi.org/10.1175/jcli-d-11-00189.1>
- 540 Young GM (2013) Climatic catastrophes in Earth history: two great Proterozoic glacial episodes. *Geol J* 48:1–21 <https://doi.org/10.1002/gj.2467> Miller, B. B. and Carter, C.: The test article, *J. Sci. Res.*, 12, 135–147, doi:10.1234/56789, 2015.